

Development of Economical Maximum Power Point Tracking System for Solar Cell

¹M.M. Rashid, ¹Riza Muhida, ²AHM Zahirul Alam, ²Habib Ullah and ¹Banna Kasemi

¹Department of Mechatronics Engineering,

²Department of Electrical and Computer Engineering, International Islamic University Malaysia.

Abstract: Photovoltaic (PV) power generation system operates under various isolation conditions, which may generate several maximum output power points on the I-V curve of the PV array and raises serious problem on Maximum Power Point Tracking (MPPT) control of the system. This research concerned the design of MPPT for photovoltaic system by using PIC controller. A MPPT unit is developed for the optimum coupling of a Photovoltaic Panel (PVP) to the battery (load) through a controlled Buck type dc-dc converter which has made the difference from the past MPPT techniques and made it cost effective. The system has high-efficiency, lower-cost and low-power consumption. Moreover it permits easy modifications. This system operates at its maximum power generation with increasing the PV output power by as much as 32-36%. This study includes the theoretical aspects and experimental results of the proposed method.

Key words: photovoltaic system, maximum power point tracking, Dc-Dc converter, PIC controller.

INTRODUCTION

Research and development on alternative energy resources have intensively been promoted due to growing concern on increasing energy demands, environmental problems and declining fossil fuels. With the cost of the solar cells decreasing, the conversion of solar energy to electric energy is increasingly becoming viable. This is particular true in a tropical country where there is abundant solar energy available throughout the year.

Photovoltaic sources are used today in many applications such as battery charging, water pumping, home power supply, swimming-pool heating systems, satellite power systems, electric vehicles, hybrid systems military and space applications, refrigeration and vaccine storage, power plants and some applications where nonlinear power source is needed. They have the advantage of being maintenance and pollution-free but their installation cost is high and they require a dc/dc or dc/ac converter for load interface. Since Photovoltaic (PV) modules still have relatively low conversion efficiency, the overall system cost can be reduced using high efficiency converters which, in addition, are designed to extract the maximum possible power from the PV module Maximum Power Point Tracking, (MPPT).

Many tracking techniques and algorithms have been developed. The Perturbation and Observation method (Femia *et al.*, 2004; 2005; Abu Tariq *et al.*, 2006), the Incremental Conductance method (Esrām *et al.*, 2007; Menniti *et al.*, 2009; Fangrui Liu *et al.*, 2009; Zhou Xuesong *et al.*, 2010) as well as Fractional Open Circuit Voltage method (Esrām *et al.*, 2007; Dorofte *et al.*, 2005) and Fractional Short Circuit Current method (Noguchi *et al.*, 2002; Esrām *et al.*, 2007;) are the most widely used. The Perturbation and Observation Method has been widely used because of its simple feedback structure and fewer measured parameters and easy to implement. The peak power tracker operates by periodically incrementing or decrementing the solar array voltage. If a given perturbation leads to an increase (or decrease) in array power, the subsequent perturbation is made in the same (or opposite) direction. In this manner, the peak power tracker, continuously hunts or seek the peak power conditions. Most maximum power trackers are based on the perturb and observe approach, implemented by a hill-climbing (Xiao and Dunford, 2004; Al-Atrash *et al.*, 2005) algorithm often on a microcontroller. However, this approach is quite complex, can be slow and thus can become 'confused' if the MPP moves abruptly.

The incremental conductance method compares the incremental conductance of the PV panel with its instantaneous conductance. The output voltage and current from the source are monitored upon which the MPPT controller relies to calculate the conductance and incremental conductance and to make its decision (to increase or decrease duty ratio output).

Mathematical of the Incremental Conductance algorithm is discussed below.

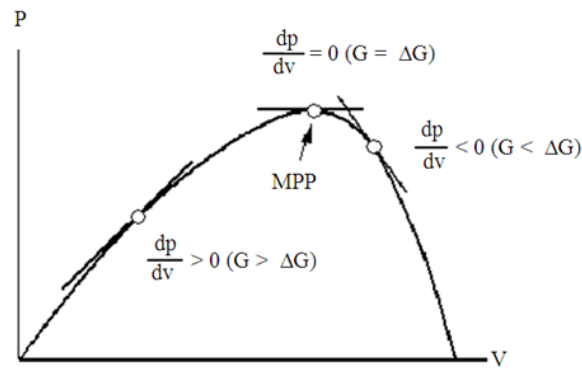


Fig. 1: The P-V curve.

The output power from the source $P = VI$ and the chain rule for the derivative of products yields:

$$dP/dV = I + V dI/dV \tag{1}$$

This implies:

$$(1/V) dP/dV = (I/V) + dI/dV \tag{2}$$

where, P , V and I are the PV array output power, voltage and current respectively. Let's define the source conductance $G = I/V$ and the source incremental conductance $\Delta G = dI/dV$. In general output voltage from a source is positive. Equation 2 explains that the operating voltage is below the voltage at the maximum power point if the conductance is larger than the incremental conductance and vice versa. The job of this algorithm is therefore to search the voltage operating point at which the conductance is equal to the incremental conductance. These ideas (Koutroulis *et al.*, 2001) are expressed by Eq. 3-5 and graphically shown in Fig. 1. Although the incremental method offers good performance under rapidly changing atmospheric conditions, high number of variables and complexity of the algorithm demand more time than P and O technique for computation and conversion, resulting in loss of energy due to not always operating at the maximum power point:

$$dP/dV > 0, \text{ if } G > \Delta G \tag{3}$$

$$dP/dV = 0, \text{ if } G = \Delta G \tag{4}$$

$$dP/dV < 0, \text{ if } G < \Delta G \tag{5}$$

The near linear relationship between VMPP and VOC of the PV array, under varying irradiance and temperature levels, has given rise to the fractional Open Circuit Voltage (VOC) method:

$$V_{MPP} \approx k_1 \cdot V_{OC} \tag{6}$$

where, k_1 is proportionality constant. Since k_1 is dependent on the characteristics of the PV array being used, it usually has to be computed beforehand by empirically determining VMPP and VOC for the specific PV array at different irradiance and temperature levels. The factor k_1 has been reported to be between 0.71 and 0.78. Once k_1 is known, VMPP can be computed using (6) with VOC measured periodically by momentarily shutting down the power converter. However, this incurs some disadvantages, including temporary loss of power.

Fractional Short Circuit Current (ISC) method results from the fact that, under varying atmospheric conditions, IMPP is approximately linearly related to the ISC of the PV array:

$$I_{MPP} \approx k_2 \cdot I_{SC} \tag{7}$$

where, k_2 is proportionality constant. Just like in the fractional VOC technique, k_2 has to be determined according to the PV array in use. The constant k_2 is generally found to be between 0.78 and 0.92. Measuring

ISC during operation is problematic. An additional switch usually has to be added to the power converter to periodically short the PV array so that ISC can be measured using a current sensor. This increases the number of components and cost.

Problem Statement and Proposed Method:

Instead of bulky system most of the methods described earlier are of high cost. In this paper the proposed system will give us a simple and cost effective with using less numbers of components. In a method proposed here, a microcontroller is used to measure the PV array output power and to change the duty cycle of dc/dc converter control signal. This method uses a low-cost, low-power consumption microcontroller, which controls a high efficiency Buck-type dc/dc converter and performs all control functions.

It is like the hill-climbing method, which seeks the optimum operating point by changing the operating point until the maximum power point is found (Jain and Agarwal, 2004; Jimenez-Brea *et al.*, 2010). Therefore this method requires power calculation using both the voltage and the current readings from the PV array. This study will discuss the design of MPPT by using hill climbing method as the control algorithm.

MATERIALS AND METHODS

Principles of Buck Converter:

The basic function of a buck converter can be seen from the circuit diagram in Fig. 2. The load, in this case a resistor is supplied via the circuit shown in the Fig. 2. It consists of a switching semiconductor T, an inductance L for storing energy, an output capacitor C₀ and a freewheeling diode D.

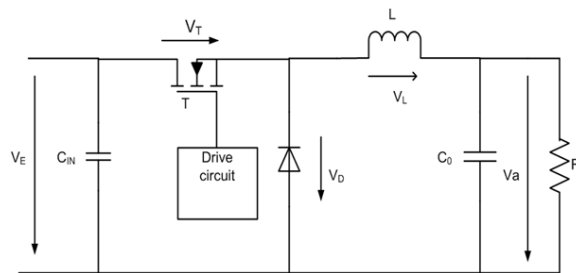


Fig. 2: Principle configuration of a buck converter with MOSFET.

First, we consider all devices to be ideal and provides a constant voltage, the output voltage is constant (C→∞) and the semiconductors are either high-impedance (open-circuit in non-conducting mode) or without any impedance (ideally conducting). Furthermore, the inductance is considered very large, but still finite. By considering steady state operation we assume that the current fed to the resistive load is equal to the average current flowing through the inductance. :

$$\bar{I}_L = \frac{\bar{V}_a}{R_{Load}} = \bar{I}_{Load} \tag{8}$$

Here the duty cycle ‘a’ describes the turn-on time t₁ of the semiconductor switch T with respect to the cycle time. T = 1/f (Fig. 5). The duty cycle a is adjusted by the control between 0 < a < 1. As soon as the switch is turned on (Fig. 3), the current flows without loss, i.e., without a voltage drop (ideal switch), through the switching device. The diode blocks, since the voltage V_D is negative.

The voltage of the inductance is equal to the difference of input voltage and output voltage:

$$v_L = V_e - V_a \tag{9}$$

The rise of current is limited by the inductance L and is proportional to the difference of input voltage and output voltage:

$$\frac{di_L}{dt} = \frac{V_e - V_a}{L} \tag{10}$$

This leads to the current waveform:

$$i_a(t) = i_a(t=0) + \frac{V_e - V_a}{L} \cdot t \quad (11)$$

As soon as the switch is turned off (Fig. 4), the current can only flow through the diode. In conducting state, there is no voltage drop across the ideal diode. Thus, the voltage drop across the inductance is equal to the negative output voltage:

$$v_L = -V_a \quad (12)$$

Hence, the current falls linearly:

$$v_L = L \frac{di_a}{dt} \Rightarrow i_a(t) = i_a(t = aT) - \frac{V_a}{L} \cdot (t - aT) \quad (13)$$

Assuming the average value of the current to be constant in the chosen stationary operational point, there cannot be an average voltage across the inductance. The positive and the negative volt-sec areas across the coil are equal, thus the following relation has to be satisfied:

$$\int_0^T v_L \cdot dt = \int_0^{aT} (V_e - V_a) \cdot dt + \int_{aT}^T -V_a \cdot dt = 0 \quad (14)$$

i.e.,

$$i_a(t=0) = i_a(t=T) \quad (15)$$

One obtains the solution of the integral:

$$(V_e - V_a) \cdot a \cdot T + (-V_a) \cdot (1 - a) \cdot T = 0 \quad (16)$$

After transformation, one obtains the following dependency of the output voltage on the input voltage and the duty cycle:

$$V_a = a \cdot V_e \quad (17)$$

According to the adjusted duty cycle, the source voltage V_e is transformed to the output side into a average voltage V_a . The voltage is equal to the source voltage V_e for $a = 1$, i.e., if the switch is always in position 1 (Fig. 3.), for $a < 1$ it is smaller respectively.

Since there are no resistive loads inside the circuit and the losses in the semiconductors are neglected, the consumed power at the input side is equal to the power delivered to the output side. Thus we obtain for the currents:

$$\bar{I}_{Load} = \frac{1}{a} \cdot \bar{I}_e \quad (18)$$

The maximum current ripple depends on the voltage V across the inductance, the inductance L and the time:

$$V = L \frac{di_L}{dt} = L \frac{\Delta i_L}{\Delta t} \quad (19)$$

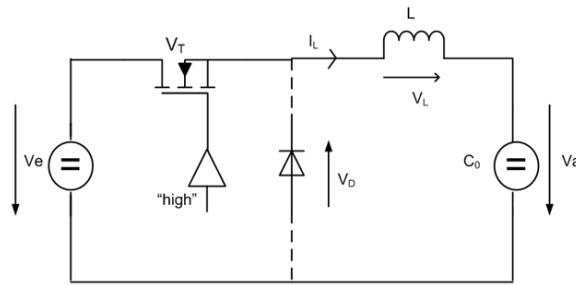


Fig. 3: Buck converter, switch turned on.

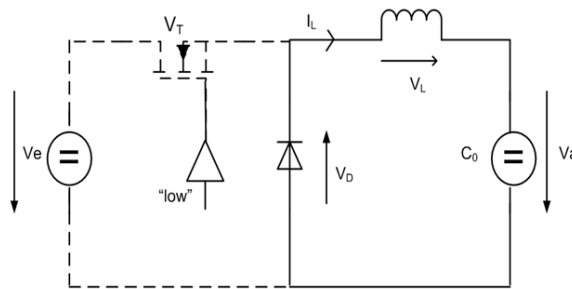


Fig. 4: Buck converter, switch turned off.

$$\Delta I_L = \frac{V_e - V_a}{L} a \cdot T = \frac{V_a}{L} (1 - a) \cdot T = \frac{V_e (1 - a) \cdot a}{L} T \quad (20)$$

The maximum current ripple is obtained for a duty cycle of $a = 0.5$.

So far, we assumed that the inductance current does not become zero at any point in time. This is only valid, if the average inductor current is larger than half the current ripple. If the average inductor current is exactly equal to half the current ripple (e.g., by means of increasing the load resistance, thus decreasing the output current), then the inductance current decays to zero for a short time. The mode of operation is called the boundary between continuous and discontinuous-conduction modes. For $V_e = \text{constant}$, these yields:

$$\bar{I}_{L, LG} = \frac{1}{2} \Delta I_L = \frac{V_e}{2L} (1 - a) \cdot a T \quad (21)$$

$$\bar{I}_{L, LG}^{\max} = \frac{1}{2} \Delta I_L^{\max} = \frac{V_e}{8 \cdot L} \cdot T \quad (22)$$

If the load current decreases further, the circuit operates in discontinuous-conduction mode (German: Lueckbetrieb, hence Index LB).

The waveform depending on the duty cycle can be seen from Fig. 6. For designing switch mode power supplies, the maximum current ripple has to be taken into account. It is also maximum for $a = 0.5$, which can be seen from (21). Due to the mandatory minimum on-

The current waveform is continuous or discontinuous depending on the parameters inductance, switching frequency and output voltage. If the current waveform is discontinuous, it is called discontinuous-conduction mode, in which one obtains:

$$aT + \epsilon T < T \quad (23)$$

Where, 'a' is defined by the falling time of the current.

According to Eq. 17-21 one obtains for the voltages and currents in discontinuous-conduction mode:

$$\frac{V_a}{V_e} = \frac{a}{a + \epsilon} \quad (24)$$

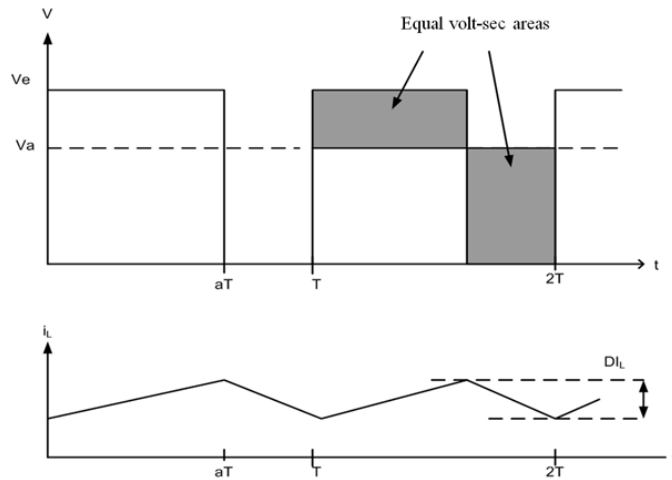


Fig. 5: Voltage-time curves over L and current curves in continuous operation.

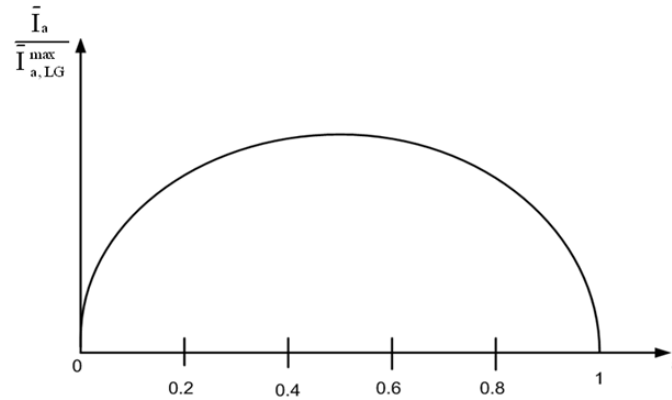


Fig. 6: Current at the boundary between continuous- and discontinuous-conduction mode depending on the duty cycle a ($V_e = \text{const}$).

period of the devices, the usable duty cycle is normally between 5 and 95%.

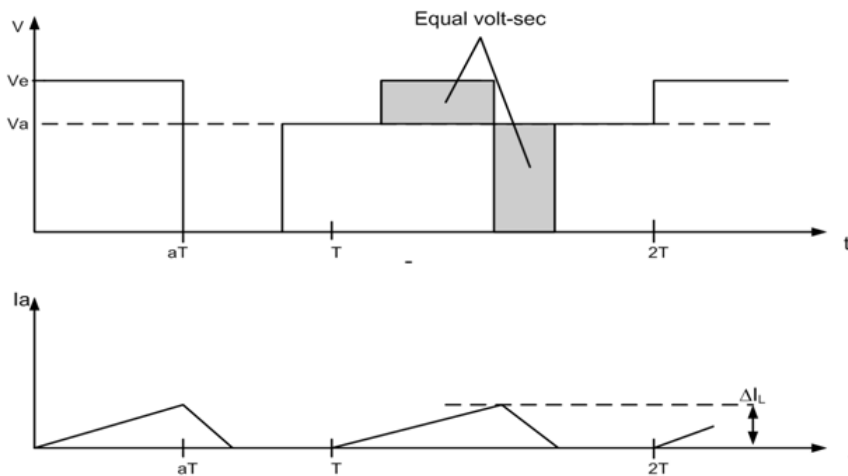


Fig. 7: Volt-sec areas and current waveform in discontinuous-conduction mode.

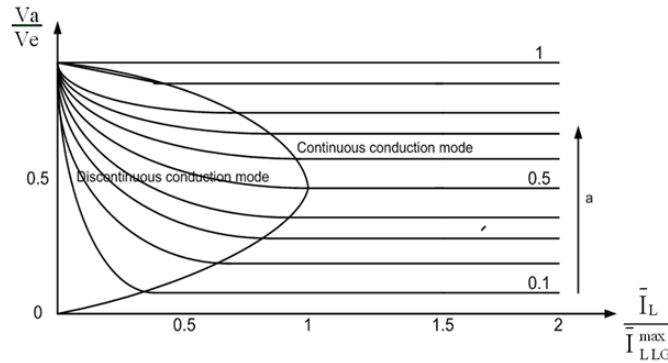


Fig. 8: Operational diagram $V_a = f(I_L)$ with duty cycle a as parameter and $V_e = \text{Const}$.

$$\bar{I}_{L, LB} = \frac{I_{L, LB}}{2} (a + \varepsilon) = \frac{\varepsilon \cdot T \cdot V_a}{2L} (a + \varepsilon) = \frac{V_e}{2L} \cdot T \cdot a \cdot \varepsilon \quad (25)$$

Equation 24 and 25 lead to:

$$\frac{V_a}{V_e} = \frac{a^2}{a^2 + \frac{1}{4} \cdot \frac{\bar{I}_{L, LB}}{\bar{I}_{L, LG}^{\max}}} \quad (26)$$

The plot of (26) is shown in Fig. 8.

Discontinuous-conduction mode only means, that there is no longer a linear relationship between output voltage and duty cycle. This can lead to the effect, that the output voltage fluctuates more than desired, e.g., because the minimum on-periods of the devices have to be kept.

Ripple of the Output Voltage:

The triangular ac current $\frac{1}{2} \Delta I_L$ (Fig. 9) leads to an alternating charge ΔQ in the ideal, i.e., lossless output capacitance C_0 . The charge and the discharge are equal (measured over one cycle in Fig. 7). The triangular area from Fig. 9 equals:

$$2\Delta Q = \frac{1}{2} \Delta I_L \cdot \frac{T}{2} = \Delta I_L \cdot \frac{T}{4} \quad (27)$$

Commonly, the type of load (e.g., a CPU) determines how large the maximum ripple of the output voltage is allowed to be. Using the relationship, one obtains:

$$C_0 \geq \frac{\Delta Q}{\Delta V_a} = \frac{\Delta I_L}{\Delta V_a} \cdot \frac{1}{8f} \quad (28)$$

Synchronous Rectifier:

For very large ratios of input voltage to output voltage (duty cycle a is very small) and for very high output currents, the losses in one lumped element, the diode, become very high.

Example:

Input voltage 12 V, output voltage 1.2 V ($a = 0.1$), output current 10 A, output power 12 W. Diode forward voltage 0.7 V (conduction interval 90%)

$$P_{\text{loss}} = 0.9 \times 10 \times 0.7 \text{ V} = 6.3 \text{ W} \quad (29)$$

This means, that half the output power is already consumed by one single element, due to the high forward voltage of the diode. In addition, the efficiency can never become higher than 65% in this case.

The synchronous rectifier represents a solution to this problem. For exactly the time interval, when the diode is conducting anyway, a MOSFET, connected in parallel having a very low $R_{DS(on)}$ is triggered. Since the voltage drop across the MOSFET is significantly lower than the forward voltage of the diode, the diode does not become conductive. Thus, the losses are reduced. In the example: $R_{DS(on)} = 0.010 \text{ Ohm}$ VMOSFET = 0.1 V:

$$P_{\text{verl}} = 0.9 \times 10 \text{ A} \times 0.1 \text{ V} = 0.9 \text{ W} \tag{30}$$

Only by this measure, the efficiency now becomes up to 93%.

Actually, the MOSFET conducts the current in the inverse direction in this circuit. However, this does not represent a technical problem, since the actual MOS-channel is always bi-directional (only one type of charge carrier). Neither the parasitic body-diode in the MOSFET nor the diodes connected in parallel on the printed circuit board interfere in this case, because the forward voltage of the diode is not reached.

Design Details of Proposed System:

The two important things in power tracker design are the switch-mode topology and the control mechanism. The tracker can be designed to either increase voltage (boost topology) or decrease voltage (buck topology) from the array going into the load.

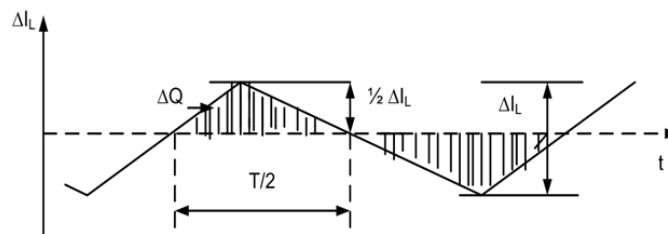


Fig. 9: Ac current flow in the capacitance C_0 .

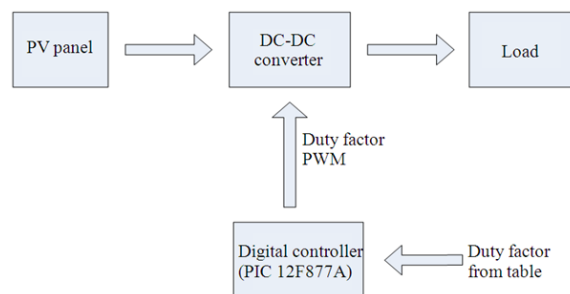


Fig. 10: System's block diagram.

The input and output currents are such that the power into and out of the tracker are equal. The control proportional to measured quantities, digitize them, process them in a micro-controller and then convert a number back to a voltage proportional to what the system believes is the maximum power point voltage of the array.

The operation of this system can be best described with reference to the block diagram shown in Fig. 10. From the block diagram the flow of the project's process can be explained. Firstly, the PV panel will receive light from the light sources. The solar cell will then generate voltage. The analog generated voltage will be fed into the controller to be processed and convert into digital signals. The conversion is done by a built-in ADC function inside the controller. The MPPT test bed is designed around the PIC16F877A microprocessor. The measured array voltages and currents are fed into dc-dc converter. The microprocessor is programmed with the MPPT algorithm to be tested. The control signal calculated by the MPPT algorithm will then generate the appropriate control signal for the DC-DC buck converter. A 12 V, 3Ah battery is used as a load for the system.

The system is based on a microcontroller which is used to measure the PV array output power and to change the duty cycle of dc/dc converter control signal. By measuring the array voltage and current, the PV array output power is calculated and compared to the previous PV array output power. Depending on the result of the comparison, the duty cycle is changed accordingly and the process is repeated until the maximum power point has been reached.

The implementation of the proposed method uses a low-cost, low-power consumption microcontroller, which controls a high efficiency Buck-type dc/dc converter and performs all control functions required by the MPPT process and battery charging (Masoum *et al.*, 2004). The main components for this project are photovoltaic panel, PIC microcontroller, dc-dc converter and battery as a load.

MPPT Algorithm:

MPPT algorithm of the hill-climbing method is used here which is based on the principle of perturbation and observation. Hill-climbing involves a perturbation in the duty ratio of the power converter and a perturbation in the operating voltage of the PV array.

The algorithm also works when instantaneous (instead of average) PV array voltage and current are used, as long as sampling occurs only once in each switching cycle. The process is repeated periodically until the MPP is reached. The system then oscillates about the MPP. The oscillation can be minimized by reducing the perturbation step size. The results will be sent out to the output port of the PIC. A timer interrupt is generated at every 100ms for initiating control action. At each duty cycle, the input voltage and input current are measured until the duty cycle is set to 100%.

Buck Converter:

The selected topology is the buck converter. It has a low number of components and only one magnetic device. A comparative study of various converters shows that buck converter requires lower device rating than other configurations. A large capacitor is used at the top to keep charging and discharging ripple to a minimum value. The choice of the converter switching frequency and the inductor value is a compromise between converter efficiency, cost, power capability and weight. For example, the higher the switching frequency, the lower the inductor core size, but the power switch losses are higher. Also, by using a large value, the peak-to-peak current ripple is smaller; requiring lower current rating power switches, but the converter size is increased substantially because a larger inductor core is required.

Depending on the load and the circuit parameters, the inductor current can be either continuous or discontinuous before the end of the switching period. When the Buck converter is used in PV applications, the input power, voltage and current change continuously with the atmospheric conditions, thus the converter conduction mode changes since it depends on them. Also, the duty cycle is changed continuously in order to track the maximum power point of the PV array.

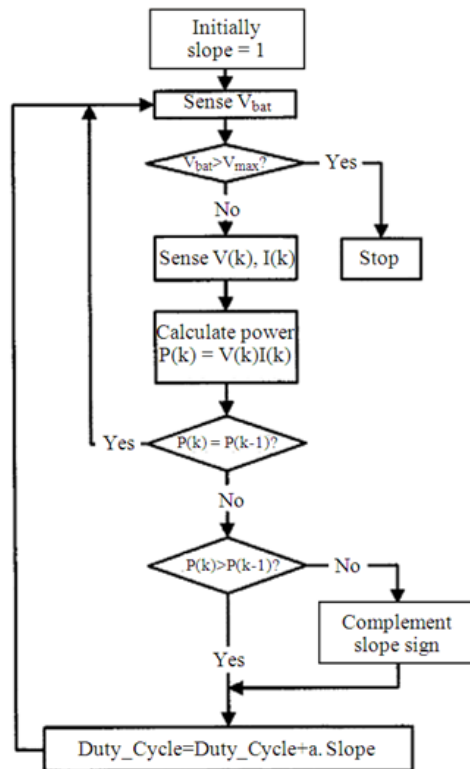


Fig. 11: MPPT control-flow chart.

Results:

Testing the Dc-dc Buck Converter:

The PV array used in this project is a multi-crystalline solar panel manufactured by BP Solar, model BP SX5M. With 36 multi-crystalline cells in series, the SX5M can charge 12 V battery efficiently with an optimal charge controller in virtually any climate. A typical application of this module, which generates nominal maximum power of 4.5 watts, includes remote telemetry, instrumentation systems, security sensors and signals. Output of the SX5M is via 4.6 m PVC jacketed 1 mm² (AWG 18-2) cable which terminates in a low-profile junction box on the module back. Epoxy-potted in box, module electrical connections are sealed against corrosion and effectively strain-relieved. The SX5M is intended for single-module applications.

A gate drive circuit switches the MOSFET between the conducting (on) and non-conducting (off) states. The converter output voltage (V_{out}) is a function of the switch duty cycle. Therefore, this control system is constructed that varies the duty cycle to cause output voltage to follow an input signal (5 V) that is supplied by portable DC power supply. From the testing (Fig. 12), it is proven that the buck converter shows a linear relationship between the control (duty cycle ratio) and output voltage as shown in Fig. 14.

Thus it easy to vary the duty ratio to get the desired output voltage, as by changing the converter's duty cycle, the input voltage (solar panel's voltage) varies accordingly.

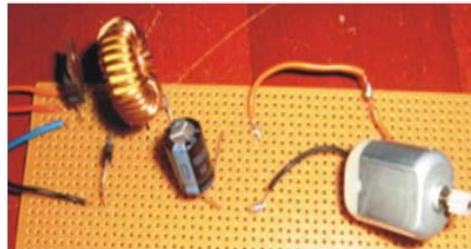


Fig. 12: DC-DC Buck Converter.



Fig. 13: Testing the buck converter.

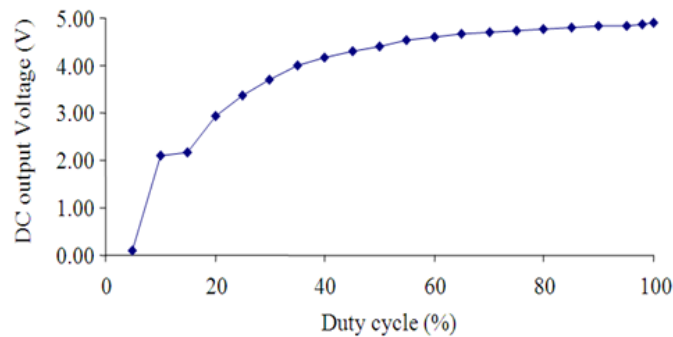


Fig. 14: buck converter Output voltage Vs duty cycle.

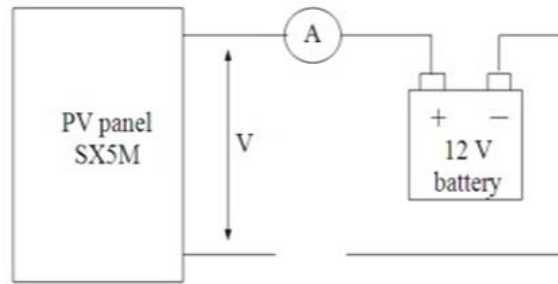


Fig. 15: Experimental setup to measure power without MPPT.

Testing the Whole Circuit:

After all the circuit related to this microcontroller has been constructed, they are connected to each other (Fig. 13) in order to test its performance. The PV array was simulated; both directly connected to the load, as shown in Fig. 15 and with PV connected to MPPT, as in Fig. 16. The results are then compared.

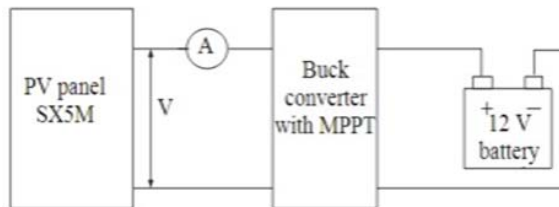


Fig. 16: Experimental setup to measure power with MPPT

Table 1: Electrical characteristics of BP SX5M.

Parameters	PV SX5
Maximum Power (Pmax) ²	4.5 W
Voltage at Pmax(Vmp)	16.5 V
Current at Pmax(Imp)	0.27 A
Warranted minimum Pmax	4 W
Short-circuit current (Isc)	0.3 A
Open-circuit voltage (Voc)	20.5 V
Temperature coefficient of Isc	-(0.065± 0.015)%/°C
Temperature coefficient of Voc	-(80±10) mV/°C
Temperature coefficient of power	(0.5±0.05) mV/°C

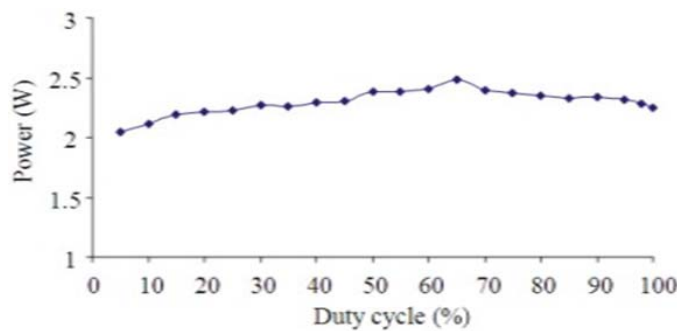


Fig. 17: Power Vs duty cycle ratio on a fine day

Results on a fine day:

In this experiment, the switching frequency is kept fixed at 2.083 kHz. The voltage and current were measured and recorded in Table 2 under various duty cycle ratios and their relationship is plotted in Fig. 17. The Results were obtained on a fine day temperature: 22-23°C.

The graph plotted in Fig. 17 shows that the maximum power is obtained during 65% duty cycle. Table 3 shows that there is an increase of 0.66W of power (increased by 36.5%) by using MPPT.

Table 2: Measurement of voltage and current on a fine day.

Duty cycle ratio (t_{on}/T) (%)	Voltage (V)	Current (A)	Power (W)
5	14.11	0.145	2.05
10	14.19	0.149	2.11
15	14.23	0.154	2.19
20	14.25	0.155	2.21
25	14.4	0.155	2.23
30	14.55	0.156	2.27
35	14.57	0.155	2.26
40	14.58	0.157	2.29
45	14.57	0.158	2.30
50	14.45	0.165	2.38
55	14.31	0.166	2.38
60	14.67	0.164	2.41
65	14.48	0.171	2.48
70	14.44	0.165	2.38
75	14.55	0.163	2.37
80	14.3	0.164	2.35
85	14.22	0.164	2.33
90	14.21	0.165	2.34
95	14.01	0.165	2.31
98	13.9	0.164	2.28
100	13.73	0.164	2.25

Table 3: Power calculation with MPPT and without MPPT (on a fine day).

Parameters	Without MPPT	With MPPT
Voltage (V)	13.98	14.48
Current (A)	0.130	0.171
Power (W)	1.82	2.48

Table 4: Measurement of voltage and current on a cloudy day.

Duty factor (t_{on}/T) (%)	Voltage (V)	Current (A)	Power (W)
10	13.01	0.049	0.64
20	13.11	0.051	0.67
30	13.18	0.051	0.67
40	13.21	0.052	0.69
50	13.21	0.053	0.70
60	13.18	0.052	0.69
70	13.19	0.051	0.67
80	13.17	0.051	0.67
90	13.17	0.051	0.67
100	13.14	0.051	0.67

Table 5: Power calculation with MPPT and without MPPT (on a cloudy day).

Parameters	Without MPPT	With MPPT
Voltage (V)	12.89	13.21
Current (mA)	40.52	52.11
Power(W)	0.52	0.69

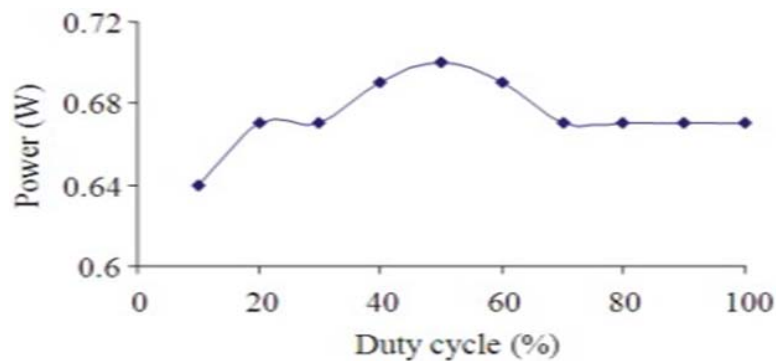


Fig. 18: Power versus duty cycle on a cloudy day.

Results on a Cloudy Day:

The voltage and current were also measured on a cloudy day and recorded in Table 4 under various duty cycle ratios and their relationship is plotted in Fig. 18. It shows that the maximum power occurs at 50% duty cycle.

Table 5 shows results taken in a cloudy day. From the measured value, we can see that there is an increase of 0.17W or 32.7% of power by using MPPT on a cloudy day.

Conclusion and Discussion:

Conventional PV energy conversion systems are bulky, expensive, provide low efficiency and are thus not suitable for small scale PV energy conversion system. In this study a novel MPPT controller is successfully developed, implemented and tested. It is used for a rapid tracking of the PV array's maximum power point to increase the efficiency and reduce the number of panels used. It has been proven as a good and reliable. Experimental results prove that the use of the proposed MPPT control increases the PV output power by as much as 32-36%. Fig. 11 shows the control algorithm loop, the execution time of which has been calculated to be less than half a millisecond, while the dc-dc converter is of the order of several milliseconds (Koutroulis *et al.*, 2001). The result shows the effectiveness of this system. It is faster and efficient as it is giving higher efficiency.

MPPT output power changes to a value that is nearly maximum power on a fine day. However, mismatch loss is great when solar radiation changes rapidly on a cloudy day. Besides that, adoption of a simple control strategy should make the MPPT more reliable. The cost of this MPPT will also be relatively low as minimum number of devices is used to execute this configuration. Additionally, because of its easy modification it can be implemented with analog circuit, with uninterruptible power system, as well as in power generation system to supply power to the electrical grid through a dc/ac converter.

REFERENCES

- Abu Tariq, M.S, Jamil Asghar, 2006. Development of microcontroller-based maximum power point tracker for a photovoltaic panel. IEEE Power India Conference, DOI: 10.1109/POWERI.2006.1632509.
- Al-Atrash, H., I. Batarseh and K. Rustom, 2005. Statistical modeling of dsp-based hill-climbing mppt algorithms in noisy environments. 20th Annual IEEE, Applied Power Electronics Conference and Exposition, APEC, (3) pp: 1773-1777. DOI: 10.1109/APEC.2005.1453286.
- Dorofte, C., U. Borup and F. Blaabjerg, 2005. A combined two-method MPPT control scheme for grid-connected photovoltaic systems," *Proc. Eur. Conf. Power Electron. Appl.*, pp: 1-10. DOI: 10.1109/EPE.2005.219714.
- Esrām, T., P.L. Chapman, 2007. Comparison of Photovoltaic Array Maximum Power Point Tracking Techniques. IEEE Transactions on Energy Conversion, 22(2): 439-449, DOI: 10.1109/TEC.2006.874230.
- Fangrui, Liu, Shanxu Duan, Fei Liu, Liu. Bangyin and Yong Kang, 2008. Variable step size inc MPPT method for PV systems. IEEE Transactions On Industrial Electronics, 55(7). DOI: 10.1109/TIE.2008.920550.
- Femia, N., G. Petrone, G. Spagnuolo and M. Vitelli, 2004. Optimizing sampling rate of P&O MPPT technique. IEEE 35th Annual Power Electronics Specialists Conference, PESC, 04(3): 1945-1949, Aachen, Germany, DOI: 10.1109/PESC.2004.1355415.
- Femia, N., G. Petrone, G. Spagnuolo and M. Vitelli, 2005. Optimization of Perturb and Observe Maximum power point tracking method. IEEE Trans. on Power Electronics, 20(4): 963-973, DOI: 10.1109/TPEL.2005.850975.
- Jain, S. and V. Agarwal, 2004. A New Algorithm for Rapid Tracking of Approximate Maximum Power Point in Photovoltaic Systems. IEEE Power Electronics Letters, 2(1): 753-762, DOI: 10.1109/LPEL.2004.828444.
- Jimenez-Brea, Emil., Andres Salazar-Llinasy, Eduardo Ortiz-Riveraz and Jesus Gonzalez-Llorentex, 2010. A Maximum Power Point Tracker Implementation for Photovoltaic Cells Using Dynamic Optimal Voltage Tracking. IEEE 25th Annual Applied Power Electronics Conference and Exposition (APEC), pp: 2161-2165, 2010. DOI: 10.1109/APEC.2010.5433536.
- Koutroulis, E., K. Kalaitzakis and N.C. Voulgaris, 2001. Development of a microcontroller-based, photovoltaic maximum power point tracking control system. IEEE Trans. Power Electron., 16(1): 46-54. DOI: 10.1109/63.903988.
- Masoum, M.A.S., S.M. Mosavi and E.F. Fuchs, 2004. A Microprocessor-controlled new class of optimal battery chargers for photovoltaic applications," *IEEE Trans. on Energy Conversion*, 19(3). DOI: 10.1109/TEC.2004.827716.

Menniti, D., A. Burgio, N. Sorrentino, A. Pinnarelli, G. Brusco, 2009. An incremental conductance method with variable step size for MPPT: Design and implementation. 10th International Conference on Electrical Power Quality and Utilisation, 2009. DOI: 10.1109/EPQU.2009.5318833”.

Noguchi, T., S. Togashi and R. Nakamoto, 2002. Short-current pulse-based maximum-power-point tracking method for multiple photovoltaic and converter module system. IEEE Trans. Ind. Electron., 49(1): 217-223, DOI: 10.1109/41.982265.

Xiao, W. and W. Dunford, 2004. A modified adaptive hill climbing mppt method for photovoltaic power systems,” IEEE 35th Annual Power Electronics Specialists Conference, 2004. PESC 04, 3: 1957-1963. DOI: 10.1109/PESC.2004.1355417

Zhou Xuesong, Song Daichun, Ma Youjie, Cheng Deshu, 2010. The simulation and design for MPPT of PV system Based on Incremental Conductance Method. IEEE WASE International Conference on Information Engineering, 2010. DOI: 10.1109/ICIE.2010.170